Biophysical Chemistry 211 (2016) 19–27

Contents lists available at ScienceDirect

Biophysical Chemistry

journal homepage: http://www.elsevier.com/locate/biophyschem

Kinetics and binding geometries of the complex between β_2-microglobulin and its antibody: An AFM and SPR study

Emilia Coppari [1], Simona Santini [1], Anna Rita Bizzarri *, Salvatore Cannistraro

Biophysics and Nanoscience Centre, Dipartimento DEB, Università della Tuscia, Viterbo, Italy

HIGHLIGHTS

- Complementary techniques are applied to study the β_2-μglobulin/antibody complex.
- Imaging, kinetics and energy landscape of the complex on substrate are characterized.
- Single molecule and in bulk results are compared.

GRAPHICAL ABSTRACT

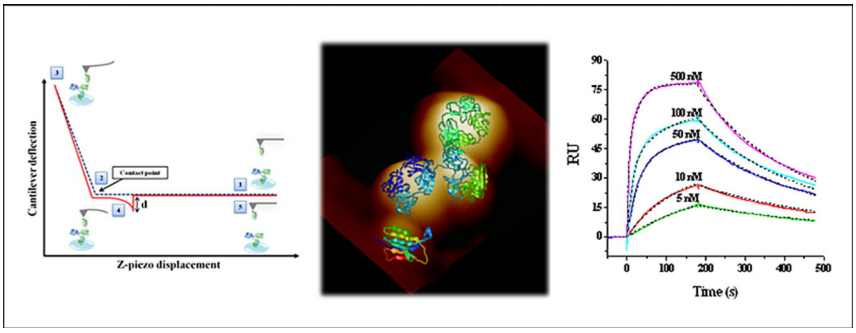

ARTICLE INFO

Article history:
Received 18 November 2015
Received in revised form 30 December 2015
Accepted 12 January 2016
Available online 15 January 2016

Keywords:
β_2-Microglobulin
Antigen–antibody biorecognition
AFM
Atomic Force Spectroscopy
Surface Plasmon Resonance

ABSTRACT

β_2-Microglobulin (B2M) is a human protein involved in the regulation of immune response and represents a useful biomarker for several diseases. Recently, anti-B2M monoclonal antibodies have been introduced as innovative therapeutic agents. A deeper understanding of the molecular interaction between the two partners could be of utmost relevance for both designing array-based analytical devices and improving current immunotherapies. A visualization at the nanoscale performed by Atomic Force Microscopy revealed that binding of B2M to the antibody occurred according to two preferred interaction geometries. Additionally, Atomic Force Spectroscopy and Surface Plasmon Resonance provided us with detailed information on the binding kinetics and the energy landscape of the complex, both at the single molecule level and in bulk conditions. Combination of these complementary techniques contributed to highlight subtle differences in the kinetics behaviour characterizing the complexes. Collectively, the results may deserve significant interest for designing, development and optimization of novel generations of nanobiosensor platforms.

1. Introduction

The formation of an antigen–antibody complex is usually preceded by a biorecognition process and plays a crucial role in the immunological response. In the last years, such a highly selective interaction has been successfully exploited for the development of immune-based, high-throughput, ultrasensitive detection of molecular biomarkers involved in human diseases [1]. Moreover, these high affinity complexes are currently employed for many clinical purposes, such as the monoclonal antibody-based targeted therapy of tumour cells [2].

An expanding interest has been recently focused on the human β_2-microglobulin (B2M), a membrane protein associated to the Major Histocompatibility Complex of Class I, involved in the regulatory

* Corresponding author at: Biophysics and Nanoscience Centre, Dipartimento DEB, Università della Tuscia, Largo dell'Università snc, 01100 Viterbo, Italy.
E-mail address: bizzarri@unitus.it (A.R. Bizzarri).
[1] These authors contributed equally to this work.

http://dx.doi.org/10.1016/j.bpc.2016.01.002
0301-4622/

mechanisms of both cellular and humoral immunities [3]. It is a useful biomarker for early diagnosis of several pathologies such as chronic inflammation, liver disease, renal dysfunction and malignancies, especially haematological cancers [4]. Interestingly, B2M represents a model in structural studies regarding the mechanisms underlying protein amyloidogenesis in neurodegenerative diseases [5].

In the last years, antiB2M monoclonal antibodies (mAbB2M), able to selectively recognize and bind B2M, have been effectively introduced as therapeutic agents for innovative treatments of B2M-associated diseases and frequently used as sensitive receptors in immunosensors [6–8]. Even if the crystallographic structure of B2M [9] and of some mAbB2Ms have been solved [10], very little is known about the structure and kinetics of their complex. In this respect, a deeper characterization of both the kinetics and the structural/geometrical features of the B2M/mAbB2M interaction could be pivotal for both designing bioactive platforms for B2M detection at low concentration and improving the current therapeutic strategies.

To this aim, we used Atomic Force Microscopy (AFM), which represents a nanotechnological tool particularly suited to investigate both the molecular details and unbinding kinetics of specific bio-complexes at the single molecule scale, without labelling, under near physiological conditions, and needing a very little amount of interacting species [11–13]. The level of structural accuracy achieved by AFM imaging enabled us to identify two distinct and recurrent molecular geometries of the antigen–antibody complex, adopted when the biopartners were adsorbed on a solid inorganic support. Moreover, Atomic Force Spectroscopy (AFS) experiments highlighted the presence of two distinct sets of kinetic parameters (dissociation/association rate constant, width of the energy barrier, dissociation/association equilibrium constant) which could reasonably be ascribable to the two interaction geometries which are imaged by AFM for the complex. The heterogeneity of the interaction and its corresponding high affinity was further assessed by Surface Plasmon Resonance (SPR) in bulk conditions. Coupling of these innovative experimental techniques allowed us to elucidate the specific biorecognition process underlying the complex formation, thus providing useful insights for improving both monoclonal antibody-based cancer therapeutic strategies and the design of array-based, label-free biosensor devices.

2. Results and discussion

2.1. AFM imaging

Fig. 1A shows a representative Tapping Mode-AFM (TM-AFM) image of isolated mAbB2M-01 molecules adsorbed on mica in air. The molecules adopt different conformations on the substrate; examples of the most frequent ones being sketched in Fig. 1B. Particularly, the characteristic Y-shaped structure of the antibodies can be immediately recognized for some molecules on the substrate, as indicated by a red-coloured circle in Fig. 1A. This conformation arises when all the three domains of the antibody bind to the surface, laying flat on the support, as also sketched in Fig. 1B (red coloured molecule). Similarly, the V-shaped morphology (blue circle in Fig. 1A) is observed when all the three domains bind the substrate, although in this case the antigen-binding fragments (Fab) are placed distant from each other forming an apex angle (Fig. 1B blue coloured antibody). In addition to these well-known antibody conformations, two other morphologies can be identified in Fig. 1A, deriving from a different tilting of the molecules on mica: a two domain morphology (yellow circle), which shows that the antibody attached to the support through the constitutive fragment (Fc) while the two Fab domains protrude from the surface and a globular-like arrangement observed when the Fab fragments are closely packed together (green circle). These last conformations are also depicted in Fig. 1B (yellow and green structures, respectively) [14–16].

The analysis of the cross section profiles (Fig. 2A) provides height values of about (1.7 ± 0.2) nm for the V- and Y-shaped morphologies (Fig. 2A) and (2.0 ± 0.2) nm for the two-domain conformations (Fig. 2B). Although these values are lower than the dimensions obtained from the X-ray, they are in a good agreement with previous AFM data obtained for similar types of IgGs and measured at analogous conditions [14,15,17]. Such a discrepancy has been explained in terms of a sample deformation caused by the tip pressure on the surface and by attractive forces ascribable to tip–sample and tip–substrate interactions, which could lead to an overcompensation of the z-piezo that introduces differences in the apparent height of the biomolecules [17–21].

Fig. 3A shows a representative image of B2M single molecules adsorbed on mica. The B2M molecules appear almost spherically shaped and characterized by a height of (0.6 ± 0.1) nm, (see the profile in Fig. 3B). Also in this case, the height is lower with respect to the X-ray data, likely due to the reasons previously mentioned.

Upon incubation of the mAbB2M-01 functionalized-substrate with a B2M solution, the biorecognition process between the partners leads the biomolecular partners to arrange into conformations which are ascribable to their complex. Fig. 4A shows one frequently found interaction mode consisting in a V-shaped antibody binding a single B2M molecule. The partners are laterally disposed, interacting each other and with the substrate. The molecular structures of the two partners have been superimposed on a magnification of the AFM 3D images of both the antibody and the B2M molecules (Fig. 4B). Since the X-ray structure of mAbB2M-01 is unknown, we have used the very similar structure of an Immunoglobulin G2a (IgG2a) isotype antibody (Protein Data Bank file, 1IGT). The quite good matching of the 3D complex could suggest a possible molecular mechanism in which a single B2M molecule interacts with one of the two exposed Fabs of the immobilized antibody. Such a conformation might be favoured by both the interaction of the partners with the underlying substrate and the exposure of

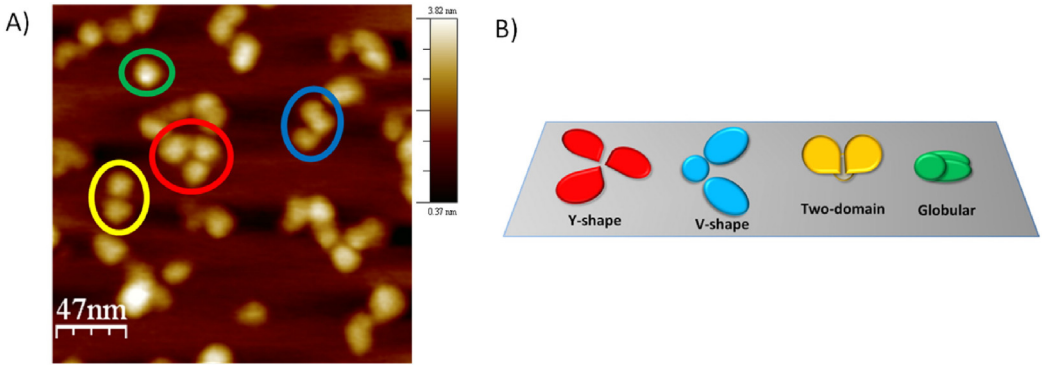

Fig. 1. A) A TM-AFM image of mAbB2M-01 molecules adsorbed on mica, recorded in air; coloured circles mark four different morphologies; B) A sketch of Y- (red) and V- (blue) shaped, two domain (yellow) and globular-like(green) morphologies as visualized in A). (For interpretation of the references to color in this figure legend, the reader is referred to the online version of this chapter.)

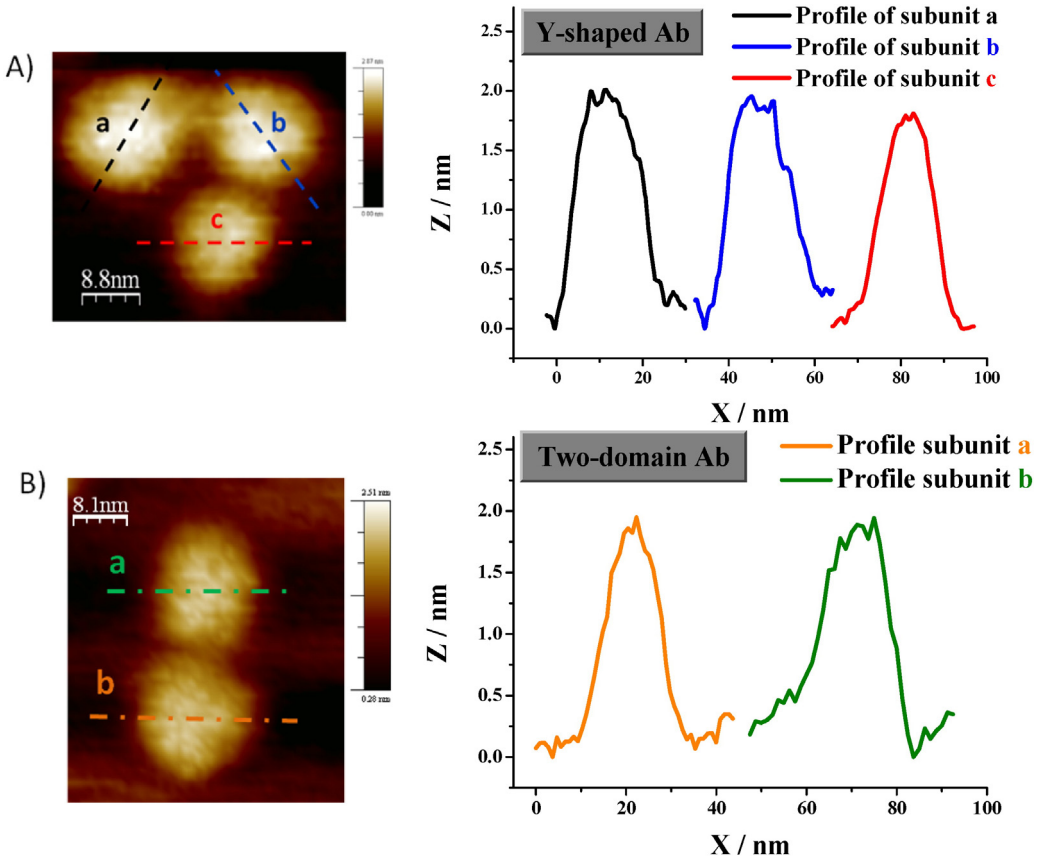

Fig. 2. Zoom-in TM-AFM images (left) of mAbB2M-01 molecules adsorbed on mica, recorded in air, and the related cross section analysis (right) of A) Y-shaped and B) two-domain morphologies.

an aromatic amino acid rich region of the antibody to the antigen, as reported for other Ag–Ab complexes [22].

Another quite recurrent binding geometry is shown in Fig. 5A and evidenced by green-circles. A cross section profile analysis (Fig. 5C) of the spot in Fig. 5B, attributed to mAbB2M-01 oriented on the substrate in a two-domain morphology, has revealed an increase of the height from (2.0 ± 0.2) nm to (2.7 ± 0.2) nm after incubation with the antigen solution; this being consistent with an overlying of a single B2M molecule on the antibody arm. Accordingly, the increased number of bright spots over the surface is also indicative of the formation of the complex (Fig. 5A).

Collectively, our results suggest that the interaction of the mAbB2M-01 with the substrate leads to the selection of specific antibody conformations, the most recurrent of which being the V-shape and the two-domain morphologies. The adopted conformations do not hinder the interaction with B2M molecules which can bind to the exposed Fab domains in a one-to-one stoichiometry.

2.2. Force spectroscopy

The unbinding strength and the kinetic parameters of the complex that have been so far imaged by AFM were furtherly investigated by force spectroscopy measurements [11,13]. Fig. 6 shows a schematic representation of the AFS experiment between the antigen and its antibody; B2M is tethered to the AFM tip, located at the end of a spring cantilever, while the mAbB2M-01 is immobilized onto the substrate.

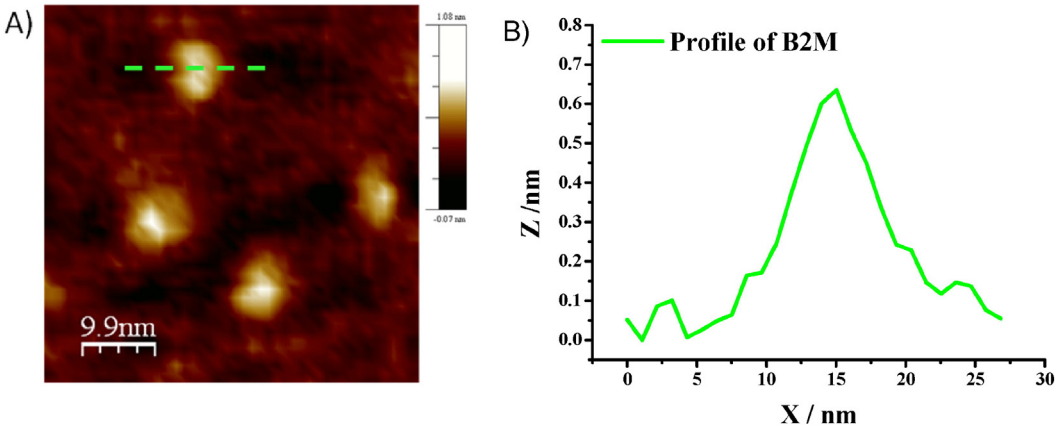

Fig. 3. A) A TM-AFM image recorded in air of B2M proteins adsorbed on mica. B) Cross section profile of the marked spot in A).

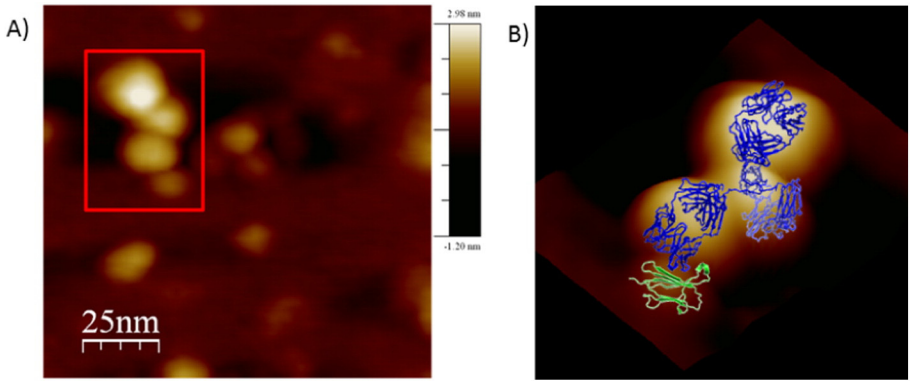

Fig. 4. A) TM-AFM image recorded in air of mAbB2M-01 adsorbed on mica after incubation with B2M, showing a spot attributed to a complex (red square). B) A zoom-in 3D topography image of the marked spot in A), interpreted as a complex formed by a V-shaped antibody binding a single molecule of B2M through one antigen-binding fragment. The molecular structures of both B2M (green) and of IgG2a (blue), have been superimposed over the 3D AFM image of the complex (images not in scale). (For interpretation of the references to color in this figure legend, the reader is referred to the online version of this chapter.)

The employed surface chemistry has been aimed at covalently coupling the biomolecules to the inorganic surfaces of the AFM tip and substrate by targeting the protein lysine amino groups in order to avoid the biomolecule detachment during the unbinding of the complex and to preserve their native structure.

During the AFS experiment, force–distance curves are recorded: the B2M-functionalized tip, starting from point 1 in Fig. 6, is approached at a constant speed to the mAbB2M-01 covered-substrate until it reaches the contact point (point 2), in the proximity of which the biorecognition process may start to take place [23]. Further approach of the tip results in an increasing overlap of the partner molecular orbitals whose repulsion yields a cantilever upward deflection which is proportional to the applied force. The approaching is stopped when a preset maximum force value is reached (point 3); thereafter the motion of the cantilever being reversed. During the retraction, adhesion forces, and/or bonds, formed in the contact phase, cause the tip to adhere to the sample up to a distance beyond the initial contact point, following a nonlinear trend which reflects the stretching of the molecular bonds [11,23]. When the spring force overcomes the interaction forces, the cantilever pulls off sharply, going to a non-contact position (point 5). Such a jump provides a measure of the unbinding force (called also rupture force) between the biomolecular partners.

Experimentally, thousands of force curves have been acquired at many distinct positions on the substrate, also varying the loading rate, r, ($r = k \cdot v$ corresponding to the product between the retraction speed of the cantilever from the substrate, v, and its spring constant, k). It is well known that the stochastic heterogeneity of the investigated biological system may result in a variety of interactions between the tip and substrate, including non-specific ones (due to contact forces, adhesions, multiple events, and so on) [13]. Since only force curves corresponding to single specific unbinding events are to be taken into consideration for further processing, a preliminary selection should be done. With such

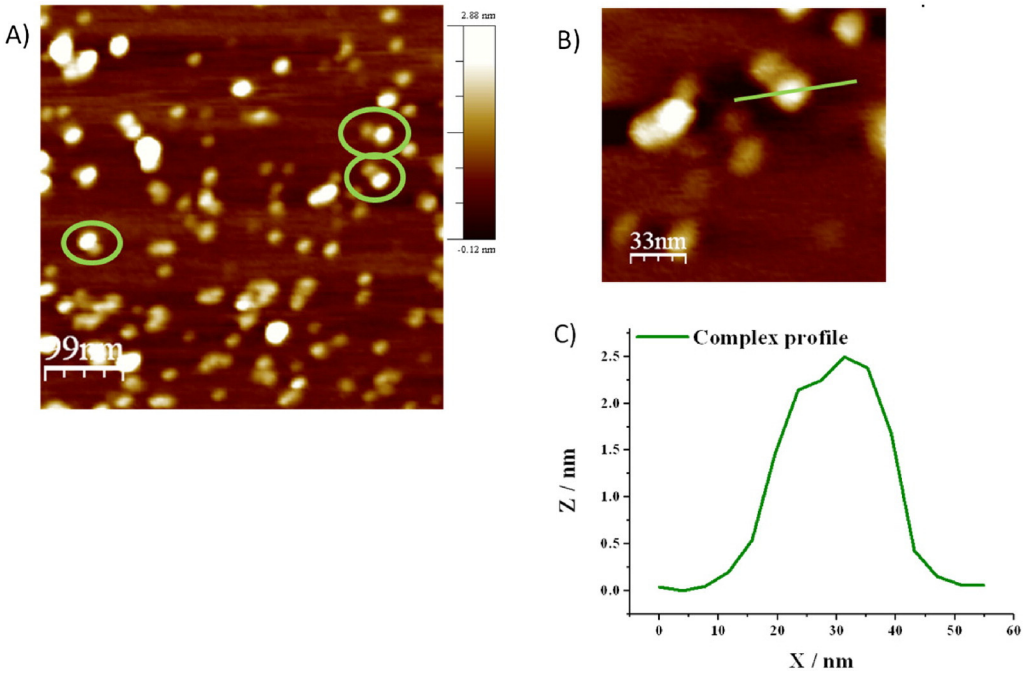

Fig. 5. TM-AFM images recorded in air of A) a mAbB2M-01/B2M sample in which spots likely corresponding to complexes are marked with green-coloured circles; B) a zoom-in image of one spot attributed to the B2M/mAbB2M-01 complex of the antibody in a two-domain morphology binding the B2M through one antigen-binding fragment; C) cross section profile of the spot shown in B). (For interpretation of the references to color in this figure legend, the reader is referred to the online version of this chapter.)

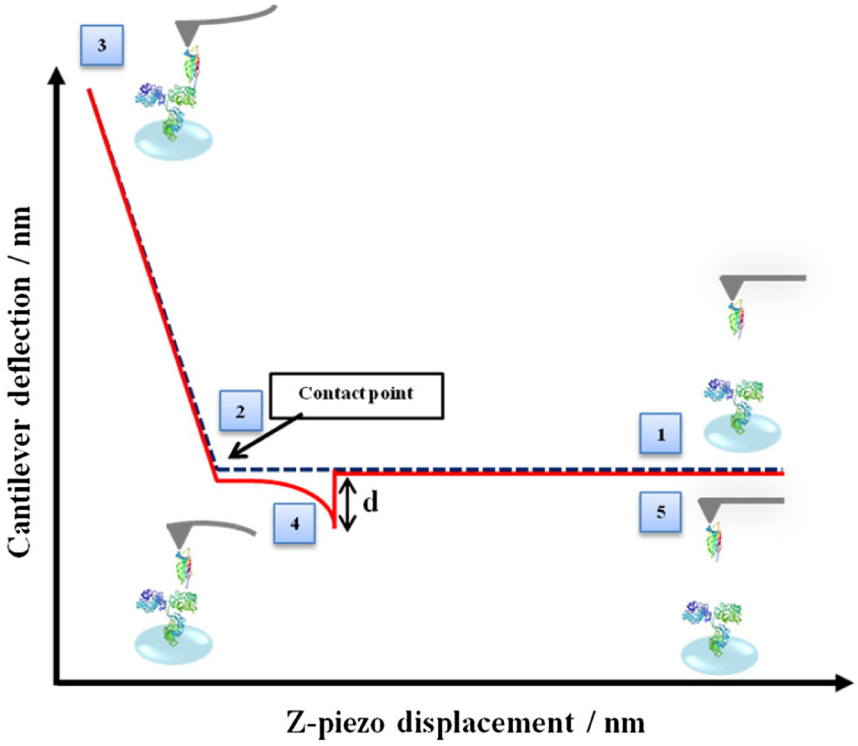

Fig. 6. A typical approach/retraction force–distance cycle of the B2M-functionalized tip and mAbB2M-01 substrate showing a specific unbinding event.

an aim, we have selected the force curves by following the procedure described in refs. [24,25], based on the analysis of the cantilever force fluctuations. Briefly, we have selected those force curves whose fluctuations exhibit: i) a 1/f noise in the approach phase before the contact point; and ii) a nonlinear trend in the retraction phase. Such an approach was indeed validated by comparing the results with those found by introducing a PEG linker between the B2M molecule and the AFM tip; with the linker stretching features having been correlated to single specific biorecognition events (see ref. [24]).

The new Fig. 7A shows an example of force curve representing a specific unbinding event. The unbinding forces extracted from these selected curves, have been collected at the five loading rates and the resulting histograms have been analysed. Fig. 8 shows the histogram corresponding to the loading rate of about 3 nN/s. We note a bi-modal distribution which can be well described in terms of two Gaussian distributions, centred at about 108 pN and 215 pN, respectively (see black lines in Fig. 8). The presence of two distributions can be put into relationship to the existence of two distinct unbinding processes, whose corresponding most probable unbinding forces (F^*) can be extracted from the position of the peaks. Similar bi-modal distributions have been also detected for the unbinding forces at the other loading rates (not shown).

Since the molecular dissociation measured by AFS takes place under the application of an external force, the system is far from the thermodynamic equilibrium with an alteration of the energy profile [26]. Therefore, to extract the kinetic and energy landscape parameters at the equilibrium, the use of suitable theoretical models is required [27–30]. Most of them take into account the unbinding process in terms of a crossing over a single, sharp barrier through the application of a time-dependent force. However, the most widely used is the model developed by Bell and Evans, which predicts a linear dependence of the most probable unbinding force, F^*, on the natural logarithm of the loading rate, r, as given by [27,28]:

$$F^* = \frac{k_B T}{x_\beta} \ln\left(\frac{r x_\beta}{k_{off} k_\beta T}\right) \quad (1)$$

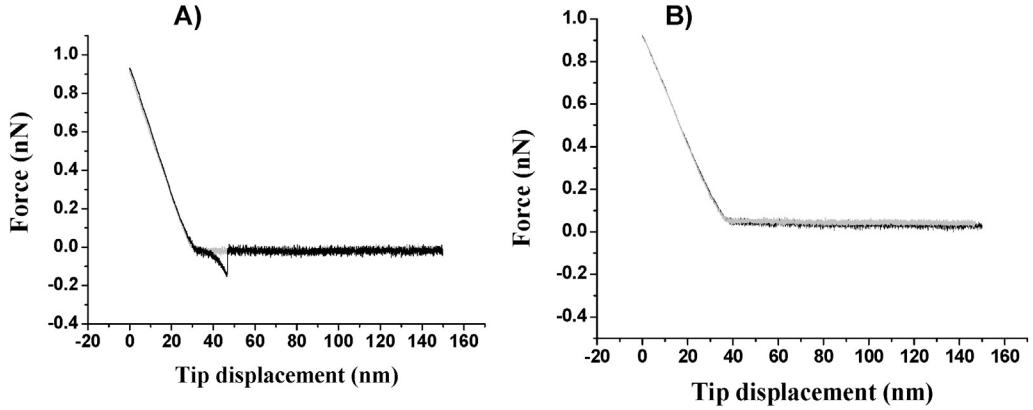

Fig. 7. Typical force curves showing a specific unbinding event (A) and without events (B). Approach curve is in grey while retrace is in black.

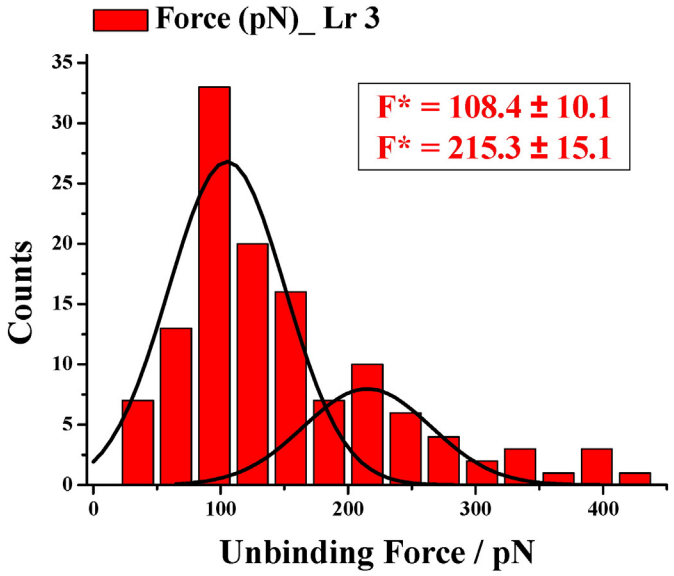

Fig. 8. Force distribution of specific unbinding events recorded by applying a loading rate of about 3 nN/s. The fitting by two Gaussian functions is used to identify the most probable unbinding force values.

where k_{off} is the dissociation rate constant at the equilibrium, x_β is the width of the energy barrier along the direction of the applied force, k_B is the Boltzmann constant and T the absolute temperature.

Fig. 9 shows the F^* values from the two peaks of the bi-modal distributions plotted versus the natural logarithm of the corresponding loading rates. In agreement with the Bell–Evans model, the presence of two linear trends is indicative of two distinct binding sites for the biomolecular partners, each of them being consistent with a single energy barrier between the bound and unbound states. Accordingly, we have fitted these data by the Bell–Evans model through Eq. (1), obtaining: $x_{\beta 1} = (0.5 \pm 0.1)$ nm and $k_{off1} = (1.8 \pm 0.5) \cdot 10^{-3}\ s^{-1}$ from the lower F^* values, and $x_{\beta 2} = (0.10 \pm 0.05)$ nm and $k_{off2} = (0.7 \pm 0.6)\ s^{-1}$ from the higher ones.

Although a rigorous evaluation of the free energy ΔG from k_{off} requires measurements as a function of the temperature, a rough estimation can be done under the assumption of a small number of involved bonds. In such a case, it can be hypothesized that the unbinding proceeds along a trajectory that resembles the thermodynamically favoured path, and the contribution of the entropic term could be neglected. Accordingly, the free energy change coincides with the

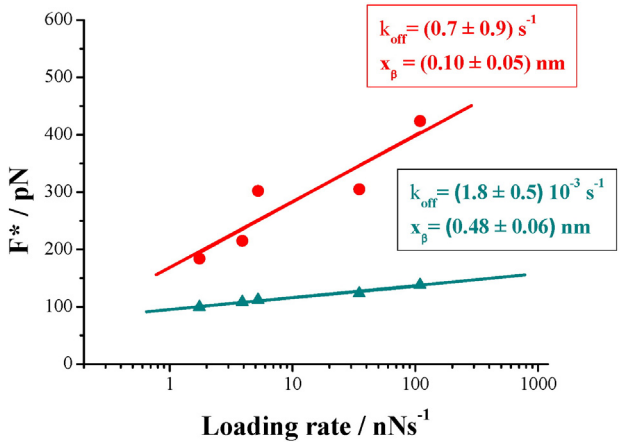

Fig. 9. The unbinding force values for the B2M/mAbB2M-01 interaction are plotted vs the natural logarithm of the loading rates. The continuous lines represent the fit of the experimental data by the Bell–Evans model (Eq. (1)). The resulting kinetic parameters, k_{off} and x_β, being also shown.

change in enthalpy and an estimation of the free energy can be obtained by the Eyring model, through the following expression [31]:

$$\Delta G_{complex} = -k_B T \ln\left(\frac{k_{off}\, h}{k_B T}\right) \quad (2)$$

where h is the Planck's constant. Accordingly, we have obtained: $\Delta G_{complex} \cong (20.8 \pm 0.2)$ kcal/mol for $k_{off1} = (1.8 \pm 0.5) \cdot 10^{-3}\ s^{-1}$ and $\Delta G_{complex} \cong (17 \pm 1)$ kcal/mol for $k_{off2} = (0.7 \pm 0.9)\ s^{-1}$. Therefore, the AFS data for the biorecognition between B2M and its monoclonal antibody suggest two different unbinding modes which are consistent with the results from the AFM imaging which shows the presence of mainly two distinct interaction sites.

To complete the kinetic profile of the interaction, we have also determined the association rate constant, k_{on}, which is mainly related to the ligand diffusion and the geometric constrains of the binding site. This parameter has been evaluated by following the procedure reported in ref. [32] and briefly described below. The interaction time between the proteins has been varied, observing an exponential increasing of the unbinding frequency (i.e., the ratio between the number of the specific events over the total recorded curves) with the contact time until reaching a maximum value. Hence, we have evaluated the time required for the half-maximal binding probability, $t_{0.5}$, of ~0.06 s and the radius, r_{eff}, of the half-sphere describing the effective volume for proteins binding (V_{eff}) of 4 nm. Then, by applying the expression $k_{on} = N_A V_{eff}/t_{0.5}$ where N_A is the Avogadro's number, we have estimated a k_{on} value of $(1.7 \pm 0.3) \cdot 10^5\ M^{-1}\ s^{-1}$. From the k_{off} and k_{on} values, we have estimated the dissociation equilibrium constant, given by ($K_D = k_{off}/k_{on}$), and giving $K_{D1} = (1.1 \pm 0.1) \cdot 10^{-8}$ M and $K_{D2} = (4.0 \pm 0.5) \cdot 10^{-6}$ M (see also Table 1). Although K_D is properly obtained from bulk measurements, its estimation can provide a further indication about the interaction properties between the partners.

These results (see Table 1) indicate the existence of a very stable conformation for the complex between the partners (mode 1) and of another one, less strong but still characterized by a rather high affinity (mode 2). Additionally, mode 1 is also characterized by a longer dissociation time, τ, provided by k_{off}, $\tau = 1/k_{off}$ with respect to the second one. It is interesting to note that the most stable complex is characterized by a larger energy barrier, x_β, (see Table 1) which can be put into relationship to the involvement of a higher number of intermolecular noncovalent bonds [33]; this being reasonably indicative of a more extended contact surface between the partners.

All these results between B2M and its monoclonal antibody confirm the formation of a stable complex consistent with those found for other systems, such as antigen–antibody, ligand–receptor, and enzyme–substrate, previously investigated by AFS [23,34]. The detection of two distinct sets of values for kinetic and thermodynamical properties can be put into relationship with two binding geometries, in agreement with the detection of two main complexes by AFM imaging. Tentatively, we might ascribe the more stable complex found by AFS data to the complex showing the antibody facing-up both the Fabs (Fig. 5). Such an interaction geometry could be favourite since the active site appears rather free from hindrances [35] and shows a larger contact surface, likely combined with a high number of intermolecular noncovalent bonds. On the whole, the AFS results point out the formation of a stable complex between one partner immobilized on the substrate and the other bound to the tip, according to two distinct geometries characterized by different kinetic and thermodynamical parameters.

2.3. SPR binding experiments

The binding kinetic between B2M and its antibody mAbB2M-01 has been also probed by SPR experiments, in order to integrate the results obtained at the single molecule level by AFS with measurements performed in bulk conditions. Furthermore, SPR allows to obtain a

Table 1
Kinetic parameters of the biorecognition process between B2M and its antibody (mAbB2M-01) as extracted from AFS experiments.

F_{unb} [a] (pN)	k_{off} (s^{-1})	τ (s)	x_β (nm)	K_D (M)	$\Delta G_{complex}$ (kcal/mol)
108	$(1.8 \pm 0.5) \cdot 10^{-3}$	555	(0.5 ± 0.1)	$(1.1 \pm 0.1) \cdot 10^{-8}$	(20.8 ± 0.2)
215	(0.7 ± 0.9)	1.4	(0.15 ± 0.05)	$(4.0 \pm 0.5) \cdot 10^{-6}$	(17 ± 1)

[a] F_{unb} values evaluated at a loading rate of 3 nN/s.

more reliable estimation of the association rate constant, k_{on}, of the interaction.

In the SPR experiment, an immobilization of the antibody molecules (mAbB2M-01, ligand) via their lysine amine groups has been chosen, obtaining thus a random orientation of the proteins onto the solid-support, similarly to the AFS experiment. The antigen (B2M, analyte) has been then fluxed free in solution over the antibody functionalized-surface by using the multi-cycle kinetic approach and the interaction has been monitored in real time through measurements of the refractive index changes.

Fig. 10A and B shows that, as far as increasing concentrations of B2M (coloured lines) are injected over the mAbB2M-01 functionalized sensor chip surface, a proportional increase of the SPR signal is observed; such an effect being due to the specific interaction of increasing amount of B2M with the mAbB2M-01 biomolecules. After 180 s of analyte injections, running buffer is fluxed over both the ligand and the reference surface and the SPR signal drops down as a consequence of the spontaneous dissociation of B2M/mAbB2M-01 complexes.

To determine the B2M/mAbB2M-01 binding kinetics, the SPR data have been analysed with two different kinetic models: i) the Langmuir 1:1 binding model and ii) the heterogeneous ligand model. The first model assumes a simple reversible bimolecular reaction between the ligand (L) and the analyte (A) [36,37], with the formation of the surface-bound ligand–analyte (LA) complex, according to the following scheme:

$$A + L \underset{k_{off}}{\overset{k_{on}}{\rightleftarrows}} LA \qquad \text{(Scheme 1)}$$

where k_{on} and k_{off} are the specific association and dissociation rate constants of the LA complex. On the other hand, the heterogeneous ligand model assumes the existence on the ligand of different binding sites for the analyte (L1 and L2), each one binding a single analyte molecule with a specific affinity [38]. The model can be described by the following scheme:

$$L_1 + A \underset{k_{off1}}{\overset{k_{on1}}{\rightleftarrows}} L_1A \quad \text{and} \quad L_2 + A \underset{k_{off2}}{\overset{k_{on2}}{\rightleftarrows}} L_2A \qquad \text{(Scheme 2)}$$

where k_{onn} and k_{offn} (n = 1 or 2) are the association and dissociation rates for the corresponding reactions, 1 or 2. Fig. 10A and B shows the best fit obtained by the 1:1 binding model and the heterogeneous ligand model, respectively (black dotted lines). From a visual inspection it is evident that the heterogeneous ligand model fits better the experimental data (Fig. 10B, black dotted lines) than the simplest 1:1 binding model. This is as also confirmed by the χ^2 values, being of ~0.6 and ~8.5 for the heterogeneous ligand model and the 1:1 binding model, respectively. The two kinetic parameter sets extracted from the heterogeneous ligand model are: $k_{on1} = (7.9 \pm 0.1) \cdot 10^4\ M^{-1}\ s^{-1}$, $k_{off1} = (49.7 \pm 0.4) \cdot 10^{-4}\ s^{-1}$; $k_{on2} = (9.5 \pm 0.1) \cdot 10^5\ M^{-1}\ s^{-1}$; $k_{off2} = (28.2 \pm 0.4) \cdot 10^{-4}\ s^{-1}$. These results indicate the presence of two binding sites characterized by very similar interaction kinetics. In particular, both of them have rather long dissociation times: $\tau_1 = 201$ s and $\tau_2 = 354$ s, respectively. Additionally, the corresponding dissociation equilibrium constants K_D, given by k_{off}/k_{on} , are: $K_{D1} = (6.3 \pm 0.1) \cdot 10^{-8}$ M and $K_{D2} = (2.9 \pm 0.1) \cdot 10^{-9}$ M, respectively. These values indicate a high affinity and fall within the range expected for the very stable and specific complexes. We note that the two values for K_D found by SPR are very close to that obtained by AFS ($K_D = (1.1 \pm 0.1) \cdot 10^{-8}$ M) for the more stable B2M/mAbB2M-01 complex conformation. The two comparable affinity profiles obtained by SPR suggest the existence of two similar interaction modes occurring when the biorecognition is monitored in bulk. These two different binding modes are characterized by very similar k_{off}, with this making them, quite reasonably, indistinguishable by AFS. On the other hand it is worth noting that the faster reaction found in AFS ($K_D = (1.1 \pm 0.1) \cdot 10^{-6}$ M) cannot be observed by SPR, since its kinetics is at the limit of the SPR detection capability (Biacore Assay Handbook — GE Healthcare Life Sciences).

3. Conclusions

Coupling of innovative techniques such as AFM imaging, AFS and SPR allowed us to outline an extensive nanoscale and kinetic characterization of the interaction between B2M and its monoclonal antibody mAbB2M-01. Particularly, the high resolution achieved by the AFM images of the single complex highlights two preferred binding

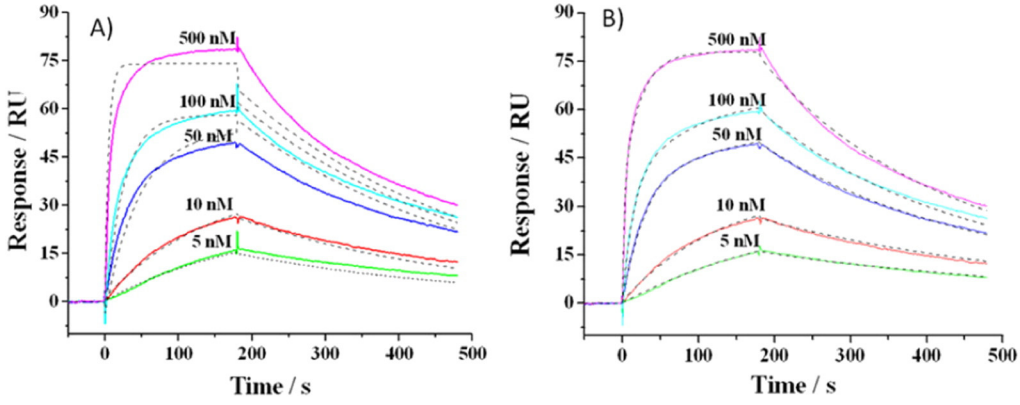

Fig. 10. SPR sensorgram resulting from the association and dissociation of B2M on mAbB2M-01-modified sensor chip surface (continuous coloured lines). A) Fit of sensorgrams by the 1:1 binding model and B) by the heterogeneous ligand model (black, dotted lines); the latter having been used to extract the kinetic parameters, k_{on}, k_{off}, and K_D (see text for details). (For interpretation of the references to color in this figure legend, the reader is referred to the online version of this chapter.)

geometries when the biorecognition occurs on a solid support. The quite good conformational matching between the molecular structures of the single partners and the AFM 3D image of their complex provides some hints on the interaction molecular mechanism. Force spectroscopy experiments confirm the formation of two different complexes with different geometries. The more stable one could presumably be associated to the complex showing the antibody in the two-domain morphology, while the other should be attributed to the complex with the mAbB2M-01 in the V-shape geometry. Furthermore, SPR binding experiments, obtained with a quite similar immobilization strategy as in AFS, but in bulk conditions, confirm the high specificity of the binding process. Comparatively, they suggest that the more stable binding mode observed by AFS could encompass the two high affinity binding modes found by SPR. In this respect, therefore, we cannot rule out the occurrence of three interaction modes when AFS experiments are carried on.

Collectively, this combined analysis provides valuable information on the energy landscape, kinetics and molecular details of the complex between B2M and its antibody helping to better understand the mechanisms underlying the biorecognition process on the solid substrate. These results could be very useful for both designing, developing and optimizing innovative biosensor platforms in which it could be taken advantage of immobilization strategies leading the antibody to assume a conformation facing up the two Fab domains, thus favouring a higher binding efficiency.

4. Experimental section

Human β_2-microglobulin (B2M) and anti-β_2-microglobulin mouse monoclonal antibody from the clone B2M-01 (mAbB2M-01) were purchased from Sigma-Aldrich (St. Louis, MO, USA) and used without further purification. Imaging and force spectroscopy measurements were performed by a NanoScope IIIa/Multimode AFM (Veeco Instruments, Plainview, NY, USA). SPR binding experiments were conducted employing a Biacore X100 instrument (GE Healthcare, Bio-Sciences AB, Uppsala, Sweden).

4.1. AFM imaging measurements

The molecules were immobilized onto freshly cleaved mica treated with a solution of $NiCl_2$ (50 mM in Milli-Q water, Millipore, Billerica, MA, USA) for 10 min. Mica was then rinsed with Milli-Q water and dried with a stream of nitrogen. Afterwards, 20 μL of a mAbB2M-01 (2 μg/mL in PBS buffer, 50 mM K_3PO_4, 150 mM NaCl, pH 7.5) or B2M (1 μg/mL, in PBS buffer) solution was incubated onto the mica, allowed to adsorb for 5 min, rinsed with water and dried with a stream of nitrogen. For imaging of the complex, a B2M solution was incubated on the mAbB2M-01 functionalized sample for 5 min, keeping the surface wet. Then, the sample was rinsed with Milli-Q water and gently dried with nitrogen. Topographical images of the proteins were carried out in air in tapping mode (TM) AFM by using a non-functionalized cantilever (NSC15 noAl, MikroMasch, Lady's Island, SC, USA) with a nominal spring constant, k_{nom}, of ~40 N/m and a resonant frequency of about 300 kHz. All the images were analysed by using the software WSxM (NanotecElectrónica S.L., Madrid, Spain) [39].

4.2. Atomic Force Spectroscopy experiments

A covalent immobilization strategy was used for preparing the AFS samples. The antigen (B2M) and antibody (mAbB2M-01) were respectively immobilized onto AFM tips and glass slides by following a procedure previously described [40]. Briefly, silicon nitride AFM tips (MSNL-10, Veeco, New York, USA) and glass slides were cleaned in acetone at room temperature and amino-functionalized by incubation in a solution of 2% (v/v) of 3-aminopropyl-triethoxysilane (APTES) (Acros Organics, Geel, Belgium) in chloroform. Then, the silanized supports were submerged in a 1% glutaraldehyde (Sigma-Aldrich, St Louis, MO, USA) solution in Milli-Q water, in order to expose aldehyde groups on the surfaces to target the outer amine groups of the protein surface. Finally, the reactive surfaces of the glass slides and tips were overnight incubated at 4 °C with a drop of a solution of mAbB2M-01 (1 mg/mL in PBS buffer) and with a B2M solution (0.1 mg/mL in PBS buffer), respectively. To passivate unreacted aldehyde groups, the functionalized tips and substrates were incubated for 5 min with a 1 mM solution of ethanolamine-HCl, pH 8.5 (GE Healthcare, Uppsala, Sweden) in Milli-Q water.

Force measurements were carried out in PBS buffer using force calibration mode AFM [41]. The used cantilever had a k_{nom} of 0.02 N/m and the effective one was determined by thermal-noise mode [42]. A ramp size of 150 nm was set up and an encounter time (interval between the approach and retraction stages) of 100 ms was established. A relative trigger of 35 nm was used to limit at 0.7 nN the maximum contact force applied by the tip on the protein monolayer. Thousands of force–distance curves were performed by maintaining constant the forward velocity at 50 nm/s and varying pulling velocities between 50 and 4200 nm/s, in order to consider the dependence of the force on the loading rates. Accordingly, the effective loading rates were calculated from the product between the pulling velocity, v, by the spring constant of the entire system, k_{syst}, that was determined from the slope of the retraction trace of the force curves immediately prior to the jump-off of an unbinding event [43], thus allowing us to take into account the effect of the molecules (i.e., proteins and/or linkers) tied to the tip. Finally, to assess that the selected force curves were reliably ascribable to specific unbinding events, two different control experiments were performed. In the first control experiment, the antibody-functionalized substrate was incubated with a solution of free B2M (30 μM in PBS buffer) and monitoring changes in unbinding frequency at loading rate 7 nN/s. Before blocking the substrate, the unbinding frequency was evaluated, finding a value of ~18%. Although this result could be considered rather low for an antigen–antibody pair [13], it might be attributed to the proteins' random orientation onto the AFM tip and substrate, which could have led to unfavourable arrangements with a reduction in the number of the binding sites. A marked reduction of the total unbinding frequency, from 18% to 6%, has been observed after B2M incubation. In the second set of control experiments, we carried out the measurements by using a bare AFM tip against the antibody-functionalized substrate, obtaining in this case a drastic reduction (down less than 1%) of the unbinding events; the most recurrent forces curve having the shape shown in Fig. 7B.

4.3. Surface Plasmon Resonance kinetic experiment

SPR experiments were carried out at 25 °C by using PBS (50 mM K_3PO_4, 150 mM NaCl, pH 7.5, surfactant P20 0.005% from GE Healthcare) as running buffer. The mAbB2M-01 proteins (ligand) were covalently coupled to a single channel of a CM5 sensor chip surface (GE Healthcare, Uppsala, Sweden) by following the standard amine coupling procedure as in ref [44]. Briefly, the dextran matrix of the sensor chip surface was initially equilibrated with running buffer and its carboxyl groups were successively activated by a mixture of N-hydroxyl-succinimide (NHS) and N-ethyl-N-(3-diethylaminopropyl) carbodiimide (EDC). mAbB2M-01 (0.025 μg/μL in 10 mM acetate buffer pH 4.5, GE Healthcare, Uppsala, Sweden) was injected for coupling reaction until 1400 RU (resonance units) immobilization level was reached, resulting from the reaction of the lysine amino groups exposed on the mAbB2M-01 surface with the functionalized sensor chip matrix. Actually, unreacted NHS-esters were blocked by a 1 M ethanolamine-HCl, (pH 8.5, GE Healthcare, Uppsala, Sweden) injection. Therefore, running buffer was fluxed over both flow cells until the baseline was stable. A control flow cell was prepared without intermediate ligand immobilization, and successively used to correct the experimental data for refractive index changes and no specific interaction.

Binding assay was performed by a multi-cycle kinetic (MCK) approach [45]. Five increasing concentrations of B2M protein (analyte) in the range of 5–500 nM were sequentially injected over both the functionalized and the reference flow cell surfaces at a flow rate of 30 μL/min for 180 s. Each analyte injection was followed by 300 s of dissociation step with a 30 μL/min flux of running buffer and then by a 20 s pulse of regeneration solution (10 mM Gly-HCl, pH 2.5, from GE Healthcare, Uppsala, Sweden) to remove the B2M molecules bound to the mAbB2M-01 antibody. The binding assay also included three start-up cycles using buffer to equilibrate the surface, as well a zero concentration cycle of analyte in order to have a blank response usable for double reference subtraction [45]. All the procedures were completely automated.

Data evaluation was performed by using the BiaEvaluation software 2.1 (GE Healthcare, BIOSciences AB, Uppsala, Sweden). The experimental curves (sensorgrams) from the functionalized surface were corrected for bulk refractive index changes, drift, and jumps due to injection needle positioning by subtracting the response obtained from the reference flow cell. The contribution of the running buffer was then subtracted. Kinetic parameters were extracted by a global fit of the corrected sensorgrams with the heterogeneous ligand model. Fits were evaluated by χ^2 value and residual plots.

Acknowledgements

This work was partly supported by a grant from the Italian Association for Cancer Research (AIRC No IG 10412) and by a PRIN-MIUR 2012 Project (No. 2012NRRP5J).

References

[1] D. Stoll, J. Bachmann, M.F. Templin, T.O. Joos, Microarray technology: an increasing variety of screening tools for proteomic research, Drug Discovery Today: Targets 3 (2004) 24–31.
[2] G.P. Adams, L.M. Weiner, Monoclonal antibody therapy of cancer, Nat. Biotechnol. 23 (2005) 1147–1157.
[3] P. Parham, T. Otha, Population biology of antigen presentation by MHC class I molecules, Science 272 (1996) 67–74.
[4] G. Coppolino, D. Bolignano, L. Rivoli, G. Mazza, P. Presta, G. Fuiano, Tumour markers and kidney function: a systematic review, BioMed. Res. Int. 2014 (2014) 1–9.
[5] J.W. Kelly, Towards an understanding of amyloidogenesis, Nat. Struct. Biol. 9 (2002) 323–325.
[6] J. Yang, Q. Yi, Killing tumor cells via their surface β2M or MHC class I molecules, Cancer 116 (2010) 1638–1645.
[7] M. Stoppini, V. Bellotti, P. Mangione, G. Merlini, G. Ferri, Use of anti-(β2 microglobulin) mAb to study formation of amyloid fibrils, Eur. J. Biochem. 249 (1997) 21–26.
[8] E. Brinda, M. Housa, A. Brandenburg, A. Wikerstal, J. Škvor, The detection of human β2-microglobulin by grating coupler immunosensor with three dimensional antibody networks, Biosens. Bioelectron. 14 (1999) 363–368.
[9] C. Rosano, S. Zuccotti, M. Bolognesi, The three-dimensional structure of β2 microglobulin: results from X-ray crystallography, Biochim. Biophys. Acta, Proteins Proteomics 1753 (2005) 85–91.
[10] J. Du, H. Yang, B. Peng, J. Ding, Structural modelling and biochemical studies reveal insights into the molecular basis of the recognition of β-2-microglobulin by antibody BBM.1, J. Mol. Recognit. 22 (2009) 465–473.
[11] P. Hinterdorfer, Y.F. Dufrene, Detection and localization of single molecular recognition events using atomic force microscopy, Nat. Methods 3 (2006) 347–355.
[12] A. Engel, D.J. Müller, Observing single biomolecules at work with the atomic force microscope, Nat. Struct. Biol. 7 (2000) 715–718.
[13] A.R. Bizzarri, S. Cannistraro, Atomic force spectroscopy in biological complex formation: strategies and perspectives, J. Phys. Chem. B 113 (2009) 16449–16464.
[14] F. Kienberger, H. Mueller, V. Pastushenko, P. Hinterdorfer, Following single antibody binding to purple membrane in real time, EMBO Rep. 5 (2004) 579–583.
[15] A. San Paulo, R. Garcia, High-resolution imaging of antibodies by tapping-mode atomic force microscopy: attractive and repulsive tip-sample interaction regimes, Biophys. J. 78 (2000) 1599–1605.
[16] S. Ido, H. Kimiya, K. Kobayashi, H. Kominami, K. Matsushige, H. Yamada, Immunoactive two-dimensional self-assembly of monoclonal antibodies in aqueous solution revealed by atomic force microscopy, Nat. Mater. 13 (2014) 264–270.
[17] N.H. Thomson, The substructure of immunoglobulin G resolved to 25 kDa using amplitude modulation AFM in air, Ultramicroscopy 105 (2005) 103–110.
[18] B. Bonanni, S. Cannistraro, Gold nanoparticles on modified glass surface as height calibration standard for atomic force microscopy operating in contact and tapping mode, J. Nanotechnol. (2005)http://dx.doi.org/10.2240/azojono0105 (Online).
[19] A. Voss, C. Dietz, A. Stocker, R.W. Starker, Quantitative measurement of mechanical properties of human antibodies with sub-10-nm resolution in a liquid environment, Nano Res. (2015)http://dx.doi.org/10.1007/s12274-015-0710-5.
[20] A. Knoll, R. Magerle, G. Krausch, Tapping mode atomic force microscopy on polymers: where is the true sample surface? Macromolecules 34 (2001) 4159–4165.
[21] D. Martinez-Martin, E.T. Herruzo, C. Dietz, J. Gomez-Herrero, R. Garcia, Noninvasive protein structural flexibility mapping by bimodal dynamic force microscopy, Phys. Rev. Lett. 106 (2011) 198101.
[22] T. Ramaraj, T. Angel, E.A. Dratz, A.J. Jesaitis, B. Mumeya, Antigen–antibody interface properties: composition, residue interactions, and features of 53 non-redundant structures, Biochim. Biophys. Acta 1824 (2012) 520–532.
[23] A.R. Bizzarri, S. Cannistraro, The application of atomic force spectroscopy to the study of biological complexes undergoing a biorecognition process, Chem. Soc. Rev. 39 (2010) 734–749.
[24] A.R. Bizzarri, S. Cannistraro, Antigen–antibody biorecognition events as discriminated by noise analysis of force spectroscopy curves, Nanotechnology 25 (2014) 1–8.
[25] A.R. Bizzarri, S. Cannistraro, 1/fα noise in the dynamic force spectroscopy curves signals the occurrence of biorecognition, Phys. Rev. Lett. 110 (2013) (048104-1-4).
[26] A.R. Bizzarri, S. Cannistraro, Dynamic Force Spectroscopy and Biomolecular Recognition, CRC Press, Boca Raton, 2012.
[27] G.I. Bell, Models for the specific adhesion of cells to cells, Science 200 (1978) 618–627.
[28] E. Evans, K. Ritchie, Dynamic strength of molecular adhesion bonds, Biophys. J. 72 (1997) 1541–1555.
[29] O. Dudko, G. Hummer, A. Szabo, Theory, analysis and interpretation of single-molecule force spectroscopy experiments, Proc. Natl. Acad. Sci. U. S. A. 105 (2006) 15755–15760.
[30] R. Friddle, A. Noy, J. De Yoreo, Interpreting the widespread nonlinear force spectra of intermolecular bonds, Proc. Natl. Acad. Sci. U. S. A. 109 (2012) 13573–13578.
[31] H. Eyring, The activated complex in chemical reactions, J. Chem. Phys. 3 (1935) 107–115.
[32] P. Hinterdorfer, W. Baumgartner, H.J. Gruber, K. Schilcher, H. Schindler, Detection and localization of individual antibody–antigen recognition events by atomic force microscopy, Proc. Natl. Acad. Sci. U. S. A. 93 (1996) 3477–3481.
[33] W. Liu, V. Montana, V. Parpura, U. Mohideen, Single-molecule measurements of dissociation rates and energy landscapes of binary trans snare complexes in parallel versus antiparallel orientation, Biophys. J. 101 (2011) 1854–1862.
[34] G. Funari, F. Domenici, L. Nardinocchi, R. Puca, G. D'Orazi, A.R. Bizzarri, S. Cannistraro, Interaction of p53 with MDM2 and azurin as studied by atomic force spectroscopy, J. Mol. Recognit. 23 (2010) 343–351.
[35] A.K. Trilling, J. Beekwilder, H. Zuilhof, Antibody orientation on biosensor surfaces: a minireview, Analyst 138 (2013) 1619–1627.
[36] P. Björquist, S. Boström, Determination of the kinetic constants of tissue factor/factor VII/factor VIIa and antithrombin/heparin using surface plasmon resonance, Thromb. Res. 85 (1997) 225–236.
[37] S. Santini, S. Di Agostino, E. Coppari, A.R. Bizzarri, G. Blandino, S. Cannistraro, Interaction of mutant p53 with p73: a surface plasmon resonance and atomic force spectroscopy study, Biochim. Biophys. Acta Gen. Subj. 1840 (2014) 1958–1964.
[38] D.J. O'Shannessy, D.J. Winzor, Interpretation of deviations from pseudo-first-order kinetic behavior in the characterization of ligand binding by biosensor technology, Anal. Biochem. 236 (1996) 275–283.
[39] I. Horcas, R. Fernandez, J.M. Gomez-Rodriguez, J. Colchero, J. Gomez-Herrero, A.M. Baro, WSXM: a software for scanning probe microscopy and a tool for nanotechnology, Rev. Sci. Instrum. 78 (2007) 013705.
[40] A.R. Bizzarri, S. Santini, E. Coppari, M. Bucciantini, S. Di Agostino, T. Yamada, C.W. Beattie, S. Cannistraro, Interaction o fan anticancer peptide fragment of azurin with p53 and its isolated domains studied by atomic force spectroscopy, Int. J. Nanomedicine 6 (2011) 3011–3019.
[41] E. Coppari, T. Yamada, A.R. Bizzarri, C.W. Beattie, S. Cannistraro, A nanotechnological, molecular-modeling, and immunological approach to study the anti-tumorigenic peptide p28 with the p53 family of proteins, Int. J. Nanomedicine 20 (2014) 1799–1813.
[42] J.L. Hutter, J. Bechhoefer, Calibration of atomic-force microscope tips, Rev. Sci. Instrum. 64 (1993) 1868–1873.
[43] R. De Paris, T. Strunz, K. Oroszlan, H.J. Guntherold, M. Hegner, Force spectroscopy and dynamics of the biotin–avidin bond studied by scanning force microscopy, Single Mol. 1 (2000) 285–290.
[44] S. Santini, A.R. Bizzarri, T. Yamada, C.W. Beattie, S. Cannistraro, Binding of azurin to cytochrome c 551 as investigated by surface plasmon resonance and fluorescence, J. Mol. Recognit. 27 (2014) 124–130.
[45] T.A. Morton, D.G. Myszka, Kinetic analysis of macromolecular interaction using surface plasmon resonance biosensors, Methods Enzymol. 295 (1998) 268–294.